Available online at www.sciencedirect.com
SCIENCE DIRECT®
Journal of Structural Biology 142 (2003) 241–246
Journal of Structural Biology
www.elsevier.com/locate/yjsbi

The binding mode of the DNA bisintercalator luzopeptin investigated using atomic force microscopy

Torunn Berge,* E. Lucy Haken, Michael J. Waring, and Robert M. Henderson

Department of Pharmacology, University of Cambridge, Tennis Court Road, Cambridge CB2 1PD, UK

Received 9 September 2002, and in revised form 20 December 2002

Abstract

The luzopeptins are DNA bisintercalating antibiotics that contain a decadepsipeptide to which are attached two quinoline chromophores. We have used atomic force microscopy (AFM) to investigate the interaction between luzopeptin B and DNA in an attempt to shed light on the binding mode of this antibiotic. AFM images provided contour lengths which were used as a direct measure of bisintercalation. Binding of luzopeptin B was investigated using two different DNA sequences, one having a GC content of 42% and the other 59%, which revealed a higher degree of bisintercalation into the DNA sequences having the lower GC content. The measured increment in contour length was found to plateau at values corresponding to binding of one drug molecule every 40 and 72 bp to the 42 and 59% GC sequences, respectively. In addition to the length increase, a higher proportion of DNA molecules displaying complex morphology was observed as the concentration of luzopeptin was increased. Such molecules were not included in the measurements of contour length. We propose that the various manifestations of complex morphology arise from both inter- and intramolecular cross-linking of the DNA caused by binding of luzopeptin, providing direct evidence of cross-linked species by AFM imaging.

Keywords: Atomic force microscopy; Bisintercalation; DNA cross-linking; Luzopeptin

1. Introduction

The luzopeptins (Fig. 1) are a group of natural antibiotics isolated from fermentation broths of *Actinomadura luzonensis* that are characterized by a cyclic decadepsipeptide core, a 10-membered peptide ring closed by an ester linkage. The cyclic scaffold, which contains D-serine as well as an unusual cyclic amino acid possessing a tetrahydropyridazine moiety, is flanked by two substituted quinoline chromophores (Huang et al., 1980; Konishi et al., 1981). These compounds have a twofold medicinal interest as they exhibit both extreme potency against tumors and activity against reverse transcriptase. They are structurally related to the quinoxaline family, comprising antibiotics such as echinomycin and triostin (Waring, 1993), and share a similar mode of DNA binding characterized by bisintercalation (Huang et al., 1982). However, luzopeptin binds to DNA at least one order of magnitude more strongly than echinomycin ($K_a \sim 10^7\,M^{-1}$) and can reduce the mobility of DNA in nondenaturing polyacrylamide gels, which has led to the speculation that luzopeptin might form covalent complexes with DNA (Fox et al., 1988). It has also been suggested that luzopeptin may be capable of forming intermolecular cross-links between DNA molecules (Huang et al., 1983), although this interpretation has been challenged (Fox and Woolley, 1990).

No strict sequence specificity has been established for luzopeptin binding, although the compound generally appears to exhibit some preference for binding to AT-rich regions in DNA. However, association with non-AT sites is certainly not excluded (Bailly et al., 2000; Fox et al., 1988). The symmetrical cyclic peptide ring is located within the minor groove, and bisintercalation is accompanied by an unwinding of the double helix by 40–50° (Searle et al., 1989; Zhang and Patel, 1991).

* Corresponding author. Fax: +44-1223-334040.
E-mail address: tb230@cam.ac.uk (T. Berge).

1047-8477/03/$ - see front matter © 2003 Elsevier Science (USA). All rights reserved.
doi:10.1016/S1047-8477(03)00015-7

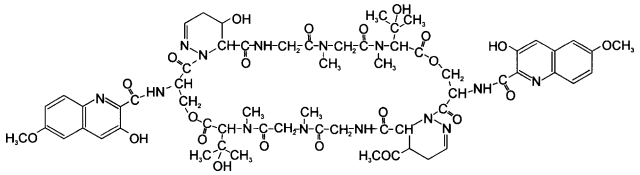

Fig. 1. The structure of luzopeptin B.

For this study, we used atomic force microscopy (AFM) to examine the binding of luzopeptin to two different DNA sequences of ~500 bp having a GC content of 42 and 59%, respectively. AFM images showing these DNA molecules with bound luzopeptin were analyzed quantitatively according to classical intercalation theory (Gale et al., 1981; Lerman, 1961). The lengthening of DNA molecules following intercalation is a result of stacking of the aromatic chromophores between base pairs and has been used previously as a readily applicable measure of drug binding using AFM images (Coury et al., 1996; Hansma et al., 1994; Lillehei and Bottomley, 2001). The well-known monointercalator ethidium bromide has been the subject of several of these studies focusing primarily on tertiary structure changes in both relaxed and supercoiled plasmid DNA (Pope et al., 2000; Utsuno et al., 2001). The single-molecule resolution of the technique is particularly suitable for detailed examination of how small molecules bind to DNA, and the present experiments were therefore undertaken in the expectation that AFM images might reveal evidence of intermolecular cross-links associated with luzopeptin binding as well as the lengthening of the double helix normally associated with intercalation.

2. Methods

2.1. DNA fragments

The DNA fragments were generated by PCR amplification of two regions of the plasmid vector pGL3-Basic (Promega, Madison, WI, USA) using two sets of primers: (1) 5′-CGTAGTGGGCCATCGCCCTG-3′ and 5′-CG ATAGAGAAATGTTCTGGCACCTGC-3′; (2) 5′ -GC AACTCGTAGGACAGGTGCC-3′ and 5′-CGGATA AGGCGCAGCGGTCG-3′ (Protein and Nucleic Acid Chemistry Facility, Department of Biochemistry, University of Cambridge). A premixed solution containing *Taq* DNA polymerase, deoxyribonucleoside triphosphates, $MgCl_2$, and reaction buffers was used (Promega Master Mix; Promega). After an initial denaturing step of 3 min at 94 °C, 35 amplification cycles were performed with the following profile: 30 s at 94 °C, 45 s at 57 °C, and 45 s at 72 °C. A final extension phase of 10 min at 72 °C was followed by a segmented cool down to 4 °C. The resulting products were DNA molecules 507 and 514 bp long having a GC content of 59 and 42%, respectively. The PCR products were identified using agarose gel electrophoresis and purified using a QIAquick PCR purification kit (Qiagen, Crawley, UK).

2.2. Luzopeptin

Luzopeptin B was a gift from Dr. M. Konishi (Bristol–Banyu Research Institute, Tokyo, Japan). Stock solutions were prepared by direct weighing and dissolved in dimethyl sulfoxide (DMSO) because of the low aqueous solubility. The antibiotic was further diluted into MilliQ water immediately before use such that the final DMSO concentration did not exceed 10%.

2.3. Sample preparation

Binding of luzopeptin to DNA was effected by mixing the antibiotic with the chosen DNA fragment at molecular ratios (luzopeptin:DNA) ranging from 10:1 to 25000:1. All samples were held at room temperature for 20 min to equilibrate. The drug–DNA complexes were then diluted in 10 mM $MgCl_2$ to a final DNA concentration of approximately 5 nM and a 50-μl droplet was deposited onto freshly cleaved ruby muscovite mica (Goodfellow, Cambridge, UK). After 10 min, the sample was gently rinsed with MilliQ water and dried under a stream of N_2 gas.

2.4. Atomic force microscopy

Imaging was performed using a multimode atomic force microscope with a Nanoscope IIIa controller (Veeco/Digital Instruments, Santa Barbara, CA, USA) operating in air and at room temperature. Commercially available cantilevers (NCH Pointprobe, Nanosensors, Norderfriedrichskoog, Germany) were used for tapping mode scanning with a root mean square amplitude of 0.7 V (~9 nm) and a drive frequency of ~300 kHz. Images were captured in height mode at a scan rate of ~1 Hz in a 512 × 512 pixel format.

2.5. Data analysis

Contour lengths of DNA molecules were determined using an image analysis program written in MatLab, version 6.00 (The MathWorks, Inc., Natick, MA, USA). Prior to analysis, all images were flattened to remove tilt and slope using the Nanoscope software function (Veeco/Digital Instruments). The program extracted digital paths for the DNA fragments based on color contrast and subsequently fitted smooth polynomial curves to the paths for measurement of contour length. Individual mean lengths were compared using the Kruskal–Wallis test performed in GraphPad InStat version 3.00 (GraphPad Software, San Diego, CA, USA). A p value less than 0.05 was considered significant. All values in

the figures and text are expressed as means ± standard error of n observations, where n represents the number of DNA fragments analyzed.

3. Results

The mode of interaction between luzopeptin and DNA was studied using AFM images of drug–DNA complexes whose contour length can be taken as a direct measure of intercalation. Each intercalated ring system should give rise to an increment in length of 0.34 nm (Gale et al., 1981; Lerman, 1961). Thus, bisintercalation of luzopeptin into DNA is expected to result in a total length increment of 0.68 nm per bound drug molecule. DNA contour lengths were extracted from the AFM images by means of computer-aided image analysis, which created digital paths based on color contrast. One such characteristic image is shown in Fig. 2A, in which a homogeneous spread of well-separated, individual DNA molecules suitable for analysis can be seen. The corresponding DNA paths extracted by the program are shown in Fig. 2B. Any DNA fragment touching either itself or other molecules was excluded from the analysis.

Because of the low aqueous solubility of luzopeptin, stock solutions were prepared in DMSO and diluted with MilliQ water immediately before use. The final concentration of DMSO in the samples never exceeded 10%. Accordingly, as a control the effect of 10% DMSO on DNA contour length was examined prior to investigating the binding of luzopeptin. The 507-bp DNA fragment prepared for imaging using pure MilliQ water in both dilution and rinse steps measured 174.9 ± 4.9 nm ($n = 107$), in good agreement with the theoretical length of B-form DNA: 172.4 nm. Use of 10% DMSO in both steps was found to produce a significant diminution in contour length down to 168.6 ± 7.0 nm ($n = 102$, $p < 0.001$). However, this effect was annulled by employing pure water in the final rinse, yielding an average length of 173.7 ± 9.8 nm ($n = 86$, $p > 0.05$).

A titration of luzopeptin B into the two different DNA fragments was carried out using molecular ratios varying from 10:1 to 25000:1. The average contour lengths were found to increase in a concentration-dependent fashion as illustrated in Fig. 3. It is evident that the interaction rapidly reaches a plateau value for both DNA fragments, with a greater number of drug molecules binding to the low-GC-content DNA. This is in agreement with previous observations (Bailly et al., 2000; Fox et al., 1988). The plateau values correspond to an average bisintercalation of ~7 and ~13 drug molecules into the ~500-bp DNA fragments, in other words, binding of drug every 72 and 40 bp to high- and low-GC-content DNA fragments, respectively. The gradient of the rising phase of the fitted curves in Fig. 3 was calculated to be 0.19 ± 0.04 (59% GC) and 0.37 ± 0.04 (42% GC) nm per drug molecule, both values significantly lower than the 0.68 nm per drug molecule

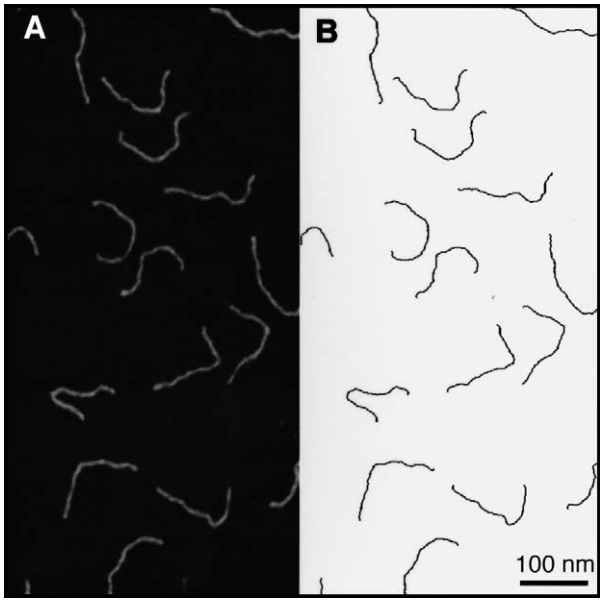

Fig. 2. AFM image showing 507-bp DNA molecules adsorbed on ruby muscovite mica in the presence of 10 mM $MgCl_2$. This AFM image of pure DNA fragments shows well-separated, individual strands (A) suitable for computer-aided analysis of contour length. The corresponding extracted digital DNA paths are shown to the right (B). Height scale (dark–light): 4 nm. Scale bar: 100 nm.

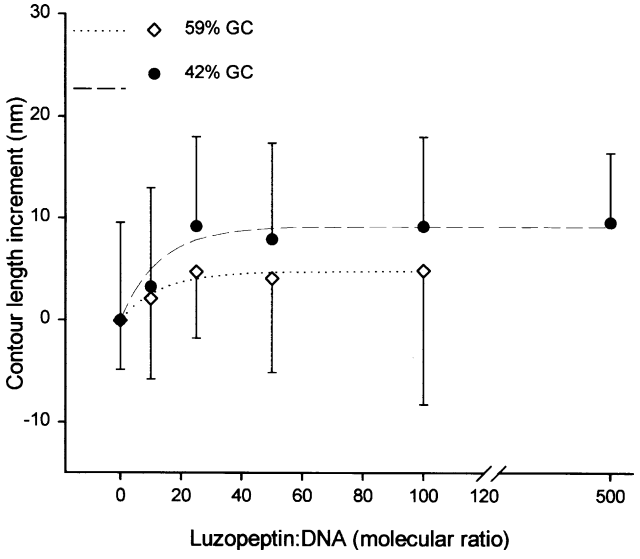

Fig. 3. The change in contour length following bisintercalation of luzopeptin into DNA fragments having GC content 42% (filled symbols) and 59% (open symbols). The plateau values reached correspond to bisintercalation of approximately 7 (59% GC) and 13 (42% GC) luzopeptin molecules. Results are expressed as means with standard deviations marked as upper (42% GC) and lower (59% GC) limits ($n = 87$–218). At a molecular ratio of 500 (luzopeptin:DNA), the fragments with the lower GC content were unsuitable for computer analysis because of a high fraction of complex conformations. $p < 0.05$ for all DNA–ligand complexes vs. control.

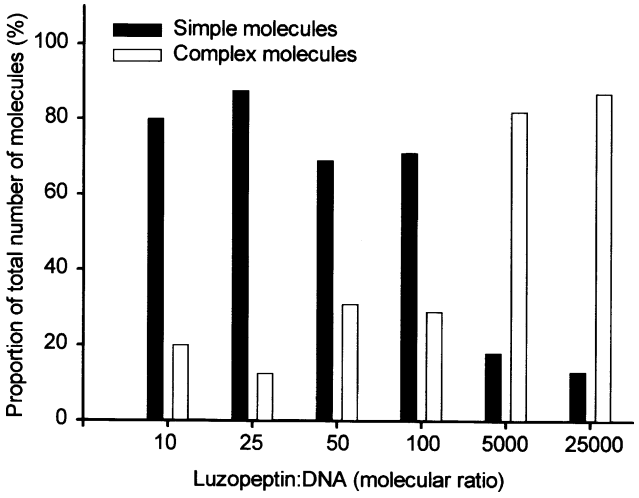

Fig. 4. Prevalence of complex as opposed to simple molecules following bisintercalation of luzopeptin. The proportion of molecules exhibiting complex morphology observed in the AFM images was found to increase with rising drug concentration. Complex molecules were excluded from the measurements of contour length. Data were extracted from images showing luzopeptin binding to DNA with 42% GC content.

expected for an ideal bisintercalation event. No doubt incomplete binding of luzopeptin is one of the contributing factors to these lower values since the proportion of free drug molecules could not be accounted for by the measurements. More important, however, is the morphology of DNA molecules considered for analysis. In addition to the increase in contour length, a rising prevalence of molecules displaying complex morphology was also evident (Figs. 4 and 5). Contour lengths were evaluated only for individual molecules displaying a simple, uncomplicated structure; consequently, the plateau value reached may not be truly representative of drug binding saturation. Previous experiments have provided conflicting evidence as to whether luzopeptin causes intermolecular cross-links between DNA molecules (Fox and Woolley, 1990; Huang et al., 1983). We now conclude that luzopeptin is indeed capable of producing cross-links between DNA double helices, for the present AFM images show a concentration-dependent increase in DNA molecules exhibiting complex conformations. Moreover, the images argue strongly that such cross-links can be formed *intra* molecularly as well, that is to say, between different portions of the same moderately long DNA molecule (Fig. 5).

4. Discussion

The mode of interaction between luzopeptin and DNA has been examined using atomic force microscopy, a technique well-suited to investigating single molecule events such as DNA–ligand interaction. The binding experiments, carried out using two different fragments having 42 and 59% GC content, respectively, are in agreement with earlier work, which showed that luzopeptin B displays a general preference for binding to AT-rich DNA sequences (Bailly et al., 2000; Fox et al., 1988). NMR studies of the complexes formed between luzopeptin and the short oligonucleotide duplexes $d(CATG)_2$ (Zhang and Patel, 1991) and $d(GCATGC)_2$ (Searle et al., 1989) have indicated that luzopeptin bisintercalates at the d(CA)–d(TG) steps. An estimate of the number of similar steps in the two sequences used here showed that the 42% GC sequence contained twice as many as the 59% GC fragment. This finding corresponds well with the average number of bisintercalated drug molecules calculated from the two titration curves given in Fig. 3, with the low-GC-content DNA binding almost twice as many luzopeptin molecules as the high-GC-content DNA (13 compared to 7 binding to ~500-bp DNA fragments).

The gradient of the rising phase in both titration curves appeared to be significantly lower than would be expected for a very tight bisintercalation event (0.68 nm per drug molecule). The image analysis program described here is, however, based on measurements of contour length and does not afford any estimate of the quantity of free drug present in the sample. The relatively large standard deviations shown in the titration curves for luzopeptin (Fig. 3) indicate a wide spread of molecules with different contour lengths present in each sample. At the very high dilutions used for AFM it is very likely that there was some degree of incomplete binding, which would certainly contribute to a lower estimate. Second, the luzopeptins are relatively large molecules and it must be considered that they could cause some buckling of the DNA helix upon intercalation. A local distortion of the helix such as buckling, a result of partial overlap between intercalated moieties and the base pairs, accommodates the intercalated quinoline chromophores without disruption of the base-pair alignment. Any such effect might also lead to drug-induced lengthening lower than the theoretical increase of 0.68 nm per bisintercalation event.

However, most notable is the increasing prevalence of complex morphology among the DNA molecules imaged by AFM as the molecular ratio of luzopeptin rises. DNA molecules of complicated appearance such as the ones shown in Fig. 5 were automatically excluded from the image analysis, so the plateau values reached in the titration curves might not truly represent binding saturation with luzopeptin. Due to the electrostatic repulsion of the negatively charged phosphate backbone, overlapping or touching DNA molecules are rarely seen in AFM images. However, these structures appeared increasingly frequently in our titration studies and could even be observed at quite low concentrations of the antibiotic.

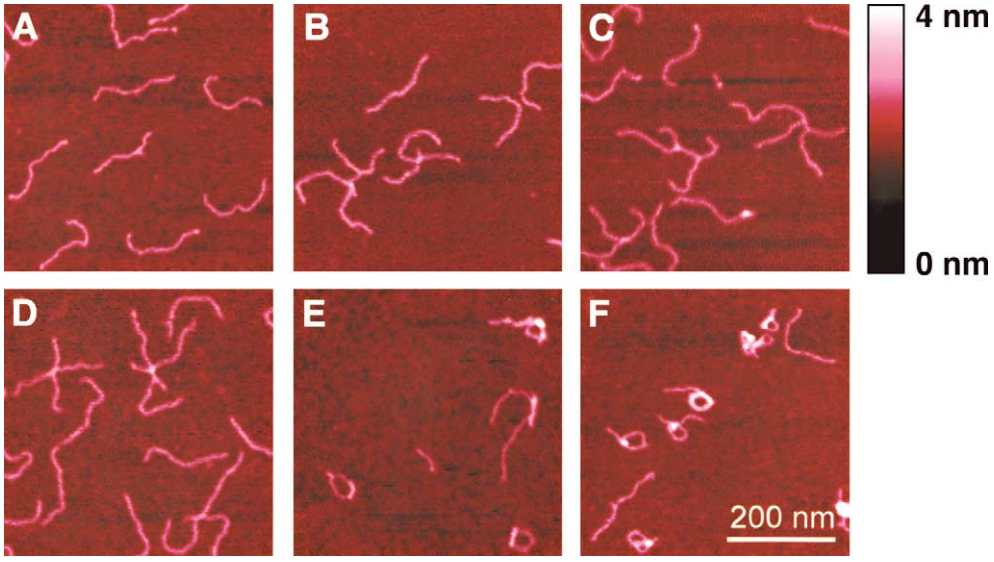

Fig. 5. The appearance of some characteristic structures observed in AFM images of luzopeptin–DNA complexes using 514-bp DNA fragments with a GC content of 42%. There is an evident increase in complexity as the concentration of luzopeptin B increases. Images were captured at molecular ratios of luzopeptin:DNA equal to (A) 0, (B) 25, (C) 50, (D) 500, (E) 5000, and (F) 25,000. Height scale (dark–light): 4 nm. Scale bar: 200 nm.

In addition to binding with the two intercalative ring systems occupying neighboring sites, bisintercalators having flexible linkers should permit binding to distant sites, both within the same duplex and on adjacent molecules. At low drug concentrations AFM images showed predominantly single, isolated DNA molecules, suggesting prototypic bisintercalating behavior. At higher drug ratios, however, the images exposed an increasing tendency for intermolecular associations to appear, in which two duplexes are linked together despite the strong electrostatic repulsion between the phosphate backbones. A further increase in the luzopeptin concentration resulted in highly complex structures, and it is likely that some of the rings or knots observed in the images (Figs. 5E and F) are produced by *intra* molecular cross-linking between distant sites on the same duplex. An increasing prevalence of apparent cross-linking with rising ratios of luzopeptin led to a larger proportion of the DNA molecules being excluded from contour length analysis as illustrated by Fig. 4.

The literature contains descriptions of various compounds that were specifically designed to promote an intermolecular mode of bisintercalation. These compounds have been used to probe the organization of DNA in three-dimensional space (Annan et al., 1992; Mullins et al., 1992), such as the structure of four-way DNA junctions (Carpenter et al., 1996). Intermolecular bisintercalation has previously been suggested as occurring when luzopeptin binds to DNA, and intermolecular cross-links seen in crystals might well revert to intramolecular cross-links in solution (Huang et al., 1983; Zhang and Patel, 1991).

The formation of intermolecular cross-links was questioned by Fox and Woolley (1990), who probed the nature of the DNA binding reaction by incubating luzopeptin with two DNA fragments of different lengths followed by separation of the reaction products on a nondenaturing polyacrylamide gel. Although smeared bands were seen, no clearly resolved species were detected corresponding to either hetero- or homodimeric products; thus it was concluded that interduplex cross-links had not been formed. At the highest ligand concentration, when the DNA should have been saturated, single bands were still not seen. We suspect that these smears are likely to contain cross-linked species such as the ones observed in the AFM images presented in Fig. 5. The variety of conformations evident in these images greatly complicates prediction of the behavior of the drug–DNA complexes in a gel, and a smeared band would perhaps be a more likely outcome than a distribution of discrete species. Marked changes in DNA mobility have also been suggested to occur not as a result of bisintercalation alone, but as a consequence of strong, possibly covalent, association between luzopeptin and DNA (Fox et al., 1988). We believe that the unusual retardation of luzopeptin-treated DNA in gels probably is attributable to the formation of intra- and intermolecular cross-links, based upon our observational evidence of complex effects by AFM imaging of luzopeptin–DNA complexes. Similar behavior has not been observed for comparable bisintercalators such as echinomycin (Fox et al., 1988; Huang et al., 1983), but the thioacetal-bridged cyclic octapeptide of echinomycin, or the disulfide-bridged ring of other quinoxaline antibiotics, is likely to be a good deal less flexible than

the unbridged decapeptide ring of the luzopeptins. Alternatively, interhelical cross-linking may just be a straightforward consequence of the stronger affinity of luzopeptin for DNA, as originally surmised.

Acknowledgments

T.B. acknowledges the support of a Research Fellowship at Emmanuel College, Cambridge. M.J.W. was supported by a grant from Cancer Research UK.

References

Annan, N.K., Cook, P.R., Mullins, S.T., Lowe, G., 1992. Evidence for cross-linking DNA by bis-intercalators with rigid and extended linkers is provided by knotting and catenation. Nucleic Acids Res. 20, 983–990.

Bailly, C., Crow, S., Minnock, A., Waring, M.J., 2000. DNA recognition by quinoline antibiotics: use of base-modified DNA molecules to investigate determinants of sequence-specific binding of luzopeptin. Nucleosides Nucleotides Nucleic Acids 19, 1337–1353.

Carpenter, M.L., Lowe, G., Cook, P.R., 1996. The structure of 4-way DNA junctions: specific binding of bis-intercalators with rigid linkers. Nucleic Acids Res. 24, 1594–1601.

Coury, J.E., McFail-Isom, L., Williams, L.D., Bottomley, L.A., 1996. A novel assay for drug–DNA binding mode, affinity, and exclusion number: scanning force microscopy. Proc. Natl. Acad. Sci. USA 93, 12283–12286.

Fox, K.R., Davies, H., Adams, G.R., Portugal, J., Waring, M.J., 1988. Sequence-specific binding of luzopeptin to DNA. Nucleic Acids Res. 16, 2489–2507.

Fox, K.R., Woolley, C., 1990. The strong binding of luzopeptin to DNA. Biochem. Pharmacol. 39, 941–948.

Gale, E.F., Cundliffe, E., Reynolds, P.E., Richmond, M.H., Waring, M.J., 1981. In: The Molecular Basis of Antibiotic Action, second ed.. Wiley, New York/London, pp. 258–401.

Hansma, H.G., Browne, K.A., Bezanilla, M., Bruice, T.C., 1994. Bending and straightening of DNA induced by the same ligand: Characterization with the atomic force microscope. Biochemistry 33, 8436–8441.

Huang, C.H., Mirabelli, C.K., Mong, S., Crooke, S.T., 1983. Intermolecular cross-linking of DNA through bifunctional intercalation of an antitumour antibiotic, luzopeptin A (BBM-928A). Cancer Res. 43, 2718–2724.

Huang, C.H., Mong, S., Crooke, S.T., 1980. Interactions of a new antitumor antibiotic BBM-928A with deoxyribonucleic acid: bifunctional intercalative binding studied by fluorometry and viscometry. Biochemistry 19, 5537–5542.

Huang, C.H., Prestyako, A.W., Crooke, S.T., 1982. Bifunctional intercalation of antitumor antibiotics BBM-p28A and echinomycin with deoxyribonucleic acid: effects of intercalation on deoxyribonucleic acid degradative activity of bleomycin and phleomycin. Biochemistry 21, 3704–3710.

Konishi, M., Ohkuma, H., Sakai, F., Tsuno, T., Koshiyama, H., Naito, T., Kawaguchi, H., 1981. BBM-928, a new antitumor antibiotic complex. III. Structure determination of BBM-928 A, B and C. J. Antibiot. (Tokyo) 34, 148–159.

Lerman, L.S., 1961. Structural considerations in the interaction of DNA and acridines. J. Mol. Biol. 3, 18–30.

Lillehei, P.T., Bottomley, L.A., 2001. Scanning force microscopy of nucleic acid complexes. Methods Enzymol. 340, 234–251.

Mullins, S.T., Annan, N.K., Cook, P.R., Lowe, G., 1992. Bisintercalators of DNA with a rigid linker in an extended configuration. Biochemistry 31, 842–849.

Pope, L.H., Davies, M.C., Laughton, C.A., Roberts, C.J., Tendler, S.J., Williams, P.M., 2000. Atomic force microscopy studies of intercalation induced changes in plasmid DNA tertiary structure. J. Microsc. 199, 68–78.

Searle, M.S., Hall, J.G., Denny, W.A., Wakelin, L.P., 1989. Interaction of the antitumour antibiotic luzopeptin with the hexanucleotide duplex d(5′-GCATGC)2: one-dimensional and two-dimensional N.M.R. studies. Biochem. J. 259, 433–441.

Utsuno, K., Tsuboi, M., Katsumata, S., Iwamoto, T., 2001. Viewing of complex molecules of ethidium bromide and plasmid DNA in solution by atomic force microscopy. Chem. Pharm. Bull. (Tokyo) 49, 413–417.

Waring, M.J., 1993. Echinomycin and related quinoxaline antibiotics. In: Neidle, S., Waring, M.J. (Eds.), Molecular Aspects of Anticancer Drug–DNA Interactions, vol. 1. Macmillan & Co., London, pp. 213–242.

Zhang, X.L., Patel, D.J., 1991. Solution structure of the luzopeptin–DNA complex. Biochemistry 30, 4026–4041.